

Polygon-free: Unconstrained Scene Text Detection with Box Annotations

Weijia Wu¹, Enze Xie², Ruimao Zhang³, Wenhai Wang⁴, Ping Luo², Hong Zhou¹

¹Zhejiang University

²University of Hong Kong Hong Kong SAR

³The Chinese University of Hong Kong, Shenzhen China

⁴Shanghai AI Laboratory

Abstract

Although a polygon is a more accurate representation than an upright bounding box for text detection, the annotations of polygons are extremely expensive and challenging. Unlike existing works that employ fully-supervised training with polygon annotations, this study proposes an unconstrained text detection system termed Polygon-free (PF), in which most existing polygon-based text detectors (e.g., PSENet [33], DB [16]) are trained with only upright bounding box annotations. Our core idea is to transfer knowledge from synthetic data to real data to enhance the supervision information of upright bounding boxes. This is made possible with a simple segmentation network, namely Skeleton Attention Segmentation Network (SASN), that includes three vital components (i.e., channel attention, spatial attention and skeleton attention map) and one soft cross-entropy loss.

Experiments demonstrate that the proposed Polygon-free system can combine general detectors (e.g., EAST, PSENet, DB) to yield surprisingly high-quality pixel-level results with only upright bounding box annotations on a variety of datasets (e.g., ICDAR2019-Art, TotalText, ICDAR2015). For example, without using polygon annotations, PSENet achieves an 80.5% F-score on TotalText [3] (vs. 80.9% of fully supervised counterpart), **31.1% better** than training directly with upright bounding box annotations, and saves **80%+** labeling costs. We hope that PF can provide a new perspective for text detection to reduce the labeling costs. The code can be found at github.com/weijiawu/Polygon-free.

1. Introduction

Scene text detection [29, 15, 37, 46, 19, 21, 36, 39, 14], which aims to locate texts in the wild, has achieved much attention in recent years because of its numerous applications, such as instant translation, image retrieval, scene parsing. Unlike other general objectives, scene text usually cannot be described accurately by the upright bounding box (see

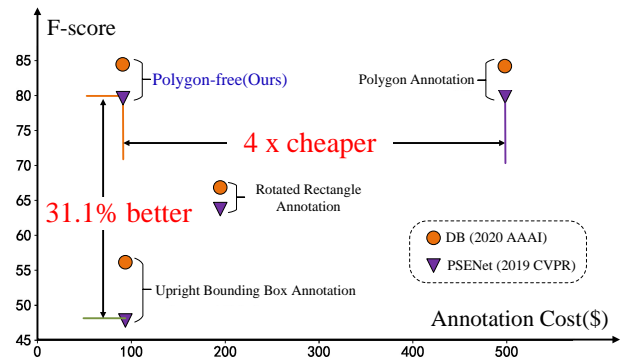


Figure 1: The performance and annotation cost for PSENet [33] and DB [16] on TotalText [3]. PSENet with Polygon-free is 31.1% better than training directly with upright bounding box annotation, 4× times cheaper than that with polygon annotation. Note that the rough cost evaluation of Total-Text is obtained by Amazon Mechanical Turk.

the example in Fig. 2 (b)), because of the diverse shapes, so most detectors using an upright bounding box annotation only achieve F-scores of below 60%, such as the 49.6% F-score for PSENet[33] on TotalText [3]. Recently, to achieve improved performance, most scene text detection methods [33, 19, 34] have utilized polygon annotation with many coordinates (see the example in Fig. 2 (d)) to capture texts with different shapes. Although the polygon annotations are more accurate than the upright bounding box annotations, the labeling cost of polygons is extremely high, limiting the wide use of this method in large-scale real-world applications [38]. According to the annotation report of the large-scale ICDAR2019-LSVT [27] dataset, 50K polygon annotations require the work of 55 personnel over five weeks, i.e., 11,000 man-hours, which is time-consuming and frustrating. By contrast, the upright bounding box annotations are more economical, and are approximately 4× cheaper than polygons annotations [3, 42], e.g., saving 80%+ annotation cost on TotalText [3], as shown in Fig. 1. This cost gap becomes larger for the large-scale benchmarks such as

ICDAR2019-LSVT [27] and ICDAR2019-Art [4]. Therefore, we aim to eliminate this obstacle by training pixel-level text detectors using upright box annotations only.

A few previous works such as BoxSup [5] and Box2Seg [13] attempted to train semantic or instance segmentation network with pseudo label from MCG [23] or GrabCut [25] based on upright bounding box annotations. One of the drawbacks of these approaches is the complicated training pipeline and a high number of hyper-parameters. Moreover, none of these methods are able to show strong weakly supervised performance. Most importantly, these methods are designed for the detection of general objects rather than for text detection. To address the text data cost issue, we first propose a simple, unconstrained system termed Polygon-free (PF) for training text detector with upright bounding box annotated data. The core idea is to transfer knowledge from low-cost synthetic data to real data to enhance the supervision information of upright bounding boxes by Attention Mechanism as inspired by the following observations.

Compared with polygon annotations, the upright bounding box is much less expensive but contains less pixel information for efficient supervision. Thus, effectively utilizing the upright bounding box annotations and boosting the text detection performance becomes critical in this case. An alternative approach is to utilize synthetic text data [7, 20] that are largely available from the virtual world, and the ground truth can be freely and automatically generated. However, many previous works [7] have shown that training directly with synthetic data degrades the performance on real data due to a phenomenon known as “domain shift” (e.g., 58.0% for EAST directly training on SynthText and testing on ICDAR2015). Unlike the existing works, motivated by the attention mechanism studies [35, 2] and BoxSup [5], we propose a Skeleton Attention Segmentation Network (SASN), and carefully design a Skeleton Attention Module based on channel attention and spatial attention to reduce the domain shift, help the network learn domain-invariant features with stronger representation power for text in a prior upright bounding box. Besides, considering the particular geometry of texts, we argue that it is more important to focus on the skeleton than on other regions. Therefore, we introduce a soft attention weight map called skeleton map and corresponding soft cross-entropy loss to enhance the representation power of the text skeleton.

To make it suitable for all detectors, the whole Polygon-free is divided into two steps: we **first** apply the synthetic data with character-level annotations to pre-train the SASN. By exploiting the text data with various geometric information (e.g., the straight and the curved data) in the training phase, SASN can effectively capture the changes of the text appearance in different scenes with the channel and spatial attention. **Then** upright bounding box annotations are used

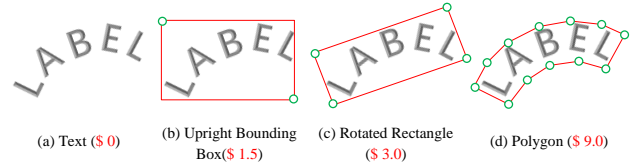


Figure 2: **Comparisons of annotation cost.** Annotation of more points is more expensive (the price of 100 text instances). Note that the data cost information is obtained from Amazon Mechanical Turk (MTurk).

to crop the text region in the real images, which are fed into SASN to generate high-quality polygon-like pseudo labels. By splicing all of these local pseudo labels, the global one would be obtained and applied to train any text detectors. As shown in Fig. 1, by using DF, PSENet [33] achieves 4× lower data cost compared with that of using polygon annotation, and obtains 31.1% F-score improvements compared with that of directly using upright bounding box annotation on Total-Text [3]. The main contributions are three folds:

(1) We first demonstrate a simple, unconstrained Polygon-free system that can train most existing text detectors with only upright bounding box annotations. This means that general detectors (e.g., PSENet [33], DB [16]) can be trained by upright bounding box annotations with no modification to the network itself.

(2) We introduce a Skeleton Attention Segmentation Network composed of three vital components (i.e., Spatial Attention, Channel Attention and Skeleton Attention) and one soft cross-entropy loss, which capturing stronger text representation and bridging the domain gap between synthetic data and real data.

(3) Polygon-free attains excellent pixel level text detection performances on several **large-scale** datasets (e.g., ICDAR2019-LSVT [27] with **50k** images and ICDAR2019-Art [4] with **10k+** curved text images). With no polygon annotations used in training, PSENet achieves **77.6%** F-score on ICDAR2019-LSVT, *even outperforming its fully supervised counterpart* (i.e., 77.4% F-score). The cost reduction for **50k** polygon annotation requiring **11,000** man-hours is highly significant.

2. Related Work

2.1. Supervised Text Detection

Scene text detection has achieved remarkable progress in the deep learning era. Previous methods [15, 45] focused on horizontal or multi-oriented text detection. CTPN [29] adopted Faster RCNN [24] and modified RPN to detect texts. EAST [46] used FCN [17] to predict the text score map, distance map and angle map. Recent works focused on curved text detection [1, 40, 21]. TextSnake [19] modeled curved text instance as a series of ordered disks and a text

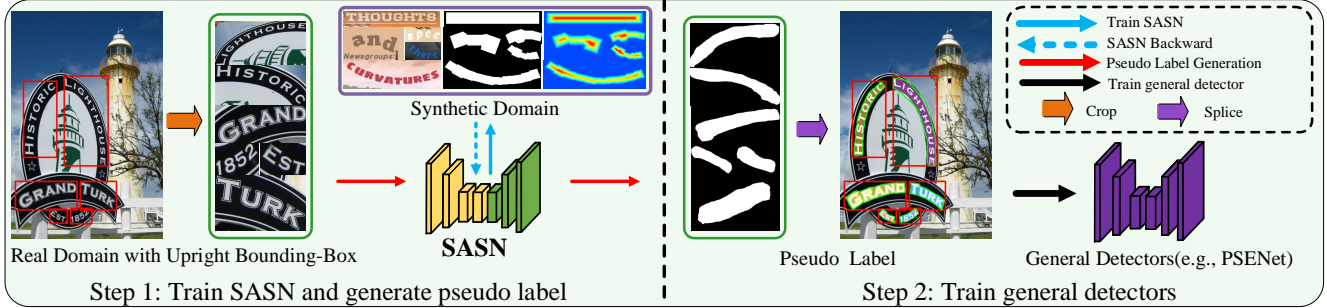


Figure 3: **Illustration of the whole Polygon-free pipeline.** Training of detectors with only upright bounding box includes two steps: (1) Train SASN (*i.e.*, Blue arrows) with synthetic data and inference on real data (*i.e.*, Red arrows) to generate polygon-like pseudo label, details shown in Fig. 4. (2) Train general detectors (*e.g.*, PSENet [33]) with the pseudo label.

center line. PSENet [33] and PAN [34] treat text instances as kernels with different scales and reconstruct the whole text instance in the post-processing. There are a few previous works [28] concerning weakly supervised text detection. WordSup[10] trains a character detector by exploiting word annotations in rich large-scale real scene text datasets.

2.2. Box-supervised Segmentation

Semantic Segmentation. To alleviate the expensive data cost problem, a few works attempted to obtain semantic mask using upright box annotations. For example, BoxSup [5] train an FCN with the pseudo labels from MCG [23], and an iterative training algorithm is used to refine the semantic masks. Box2Seg [13] employs the pseudo label generated by GrabCut [25] to supervise the training of the mask prediction model. At the same time, a per-class attention map is also predicted to make the per-pixel cross-entropy loss focus on the foreground pixels.

Instance Segmentation. Compared to semantic segmentation, utilizing box annotations to supervise instance segmentation networks is more rare. Similar to the methods for semantic segmentation, SDI [12] also utilizes the pseudo label generated by MCG [23]; however, it employs GrabCut-like algorithms to generate training labels from given bounding boxes, instead of modifying the segmentation convnet training procedure or using recursive training. Recently, BoxInst [31] train the instance segmentation framework with box supervision by introducing two loss terms for CondInst [30]. However, the above works all have one drawback, the above works are designed for common object detection and segmentation, which cannot directly be applied to text detection. Our Polygon-free can fill the gap for box-supervised text detection.

2.3. Attention Mechanism

One important property of a human visual system is that we know “what” and “where” to focus our attention in an image. Similarly, attention enables the artificial model to

focus only on the important data. The classic works based on attention, BAM [35] and CBAM [35] increase the accuracy of the classifier by utilizing both 1D channel and 2D spatial self-attention maps. CBAM learns better feature representation by refining features with attention maps obtained from two different dimensions: channel and spatial. BAM constructs hierarchical attention at bottlenecks, and it is trainable in an end-to-end manner jointly with any feed-forward models. Considering the particular geometry of texts, we propose a novel skeleton attention map to replace the attention map in CBAM and carefully design a Skeleton Attention Segmentation Network with the channel and spatial attention to bridge the domain shift.

3. Approach

3.1. Polygon-free System

Inspired by the classic weakly-supervised work Box-Sup [5] that segmenting with upright bounding boxes, we propose an unconstrained weakly supervised method, termed Polygon-free (PF), which can achieve competitive accuracy with low-cost upright bounding box annotations for text detection. As shown in Fig. 3, PF utilizes a novel proposed Skeleton Attention Segmentation Network (SASN), which is shown in Fig. 4, to generate polygon pseudo labels based on the given upright bounding box annotations. This process consists of two steps: (1) In the first step (see the blue arrows in Fig. 3), we train SASN with almost free synthetic data based on character annotation. And then, the box-level annotations are utilized to crop the real image, which are fed into the SASN for generating polygon-like pseudo labels (see red arrows in Fig. 3). (2) By splicing all of the local pseudo labels, the global pseudo label is obtained. In this way, upright bounding box annotations can be converted to high-quality polygon pseudo labels. General detectors (*e.g.*, PSENet [33]) trained on these pseudo labels can achieve almost the same performance as those trained on original polygon annotations.

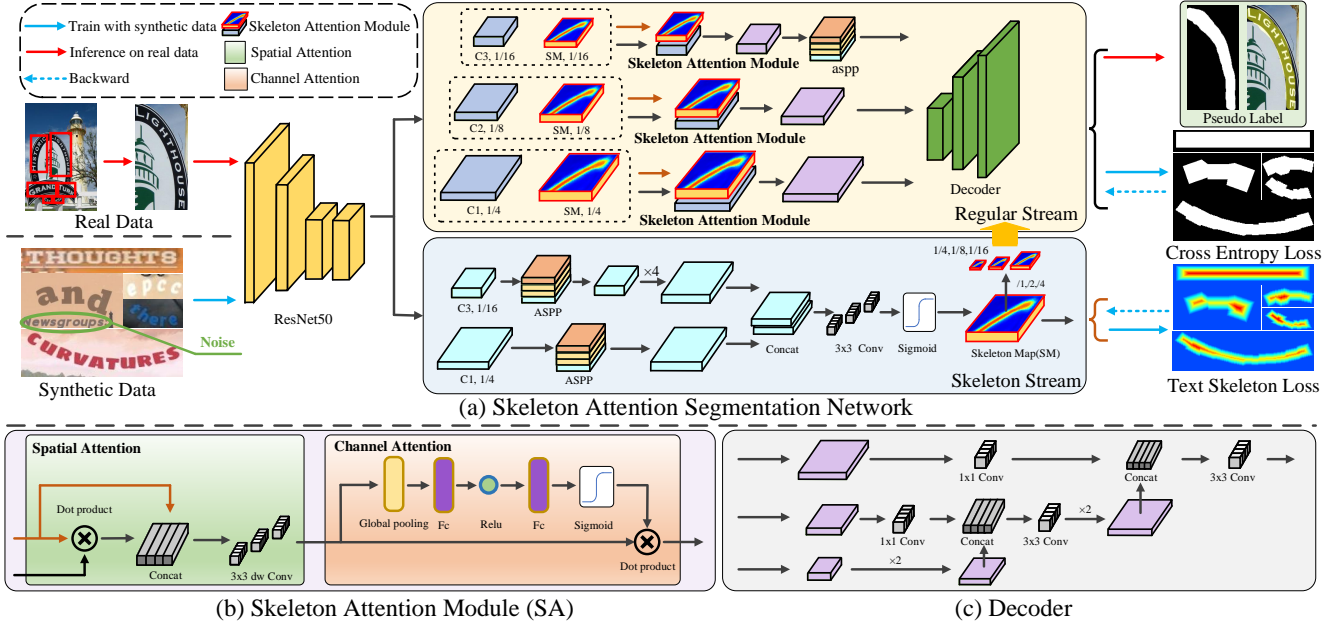


Figure 4: **The network architecture of Skeleton Attention Segmentation Network.** (a) SASN is composed of two streams: regular stream and skeleton stream. (b) Skeleton Attention Module is composed of channel attention and spatial attention, which refine the input feature map by weighting with text skeleton map. (c) The detailed structure of the Decoder.

3.2. Skeleton Attention Segmentation Network

A Probabilistic Perspective for Skeleton Attention.

Although synthetic data such as SynthText [7] can be automatically generated with diversified appearance, the model trained with only synthetic data generally cannot obtain satisfactory performance on real scenes due to the existence of domain shift, *e.g.*, 58.0% F-score for EAST [46] directly training on SynthText [7] and testing on ICDAR2015 [11]. Compared with training on original training set of ICDAR2015 (*i.e.*, 76.4% F-score), there exists a performance gap 18.4%. The prior upright bounding box can provide much prior knowledge, but there are still severe domain shifts. Here, we provide a probabilistic perspective for this problem. The segmentation problem can be viewed as learning the posterior $P(M|I)$, where I refers to the image representation and M is the predicted mask of text instances. Let us denote the joint distribution of benchmark for segmentation as $P(M, I)$, and use $P_S(M, I)$ and $P_R(M, I)$ to denote the synthetic domain joint distribution and the real domain joint distribution (see the left in Fig. 3), respectively. In the presence of a domain shift, $P_S(M, I) \neq P_R(M, I)$. Using the Bayes's Formula, the joint distribution can be decomposed as:

$$P(M, I) = P(M|I)P(I), \quad (1)$$

Similar to the classification problem [32], we make the covariate shift assumption that the conditional probability

$P(M|I)$ is the same for the two domains, and the domain distribution shift is caused by the difference on the marginal distribution $P(I)$. In the text segmentation task, the image representation I is actually the feature map from the network. Therefore, to handle the domain shift problem, we try to enforce the marginal distribution from two domains to be the same (*i.e.*, $P_S(I) = P_R(I)$) by learning better discriminative text features. Inspired by the CBAM [35], we carefully design the Skeleton Attention Module (SAM) to learn domain invariant features, focusing on important features and suppressing unnecessary ones from two aspects: channel attention and spatial attention (see the left notes and (b) in Fig. 4). In addition, strong noise interference also exists in real data. For example, two texts in one upright bounding box for which we only require the body text as the foreground, as illustrated in the Fig. 4 (a) with the green circle. Thus, considering the special geometry of texts, we argue that the skeleton is more important than the other regions, particularly in the case of existing other text interference. Therefore, we introduce a soft attention weight map termed skeleton map to enhance the representation power of the text skeleton.

Network Architecture. As presented in Fig. 4 (a), we use ResNet50 [9] as the backbone network for the SASN, and extract three levels of features (*i.e.*, $C1, C2, C3$) from different downsampled scales (*i.e.*, $1/4, 1/8, 1/16$). After that, the skeleton stream fuses $C1$ and $C3$ to predict

the skeleton attention map, and the Atrous Spatial Pyramid Pooling module (ASPP) is used to enlarge the receive field. The skeleton attention map is downsampled to make it suitable for multi-scale feature maps. At the same time, the regular stream refines multi-scale features (*i.e.*, $C1, C2, C3$) by applying the Skeleton Attention Module. Finally, $C1, C2, C3$ are fed into the Decoder, as shown in Fig. 4 (c). The C3 and C2 are first fused by up-sampling and concatenation. The fused feature map is further up-sampled to fuse with $C1$ in the same approach.

3.3. Skeleton Attention Module

Spatial and Channel Attention. Fig. 4 (b) illustrates the details of the two attention methods. Given an intermediate feature map $F \in \mathbb{R}^{C \times H \times W}$ (*i.e.*, the orange input in Fig. 4 (b)) and an skeleton map $F_{sm} \in \mathbb{R}^{C \times H \times W}$ (*i.e.*, the black input in Fig. 4 (b)), spatial attention is first utilized to focus on “where” is the text skeleton by multiplication and concatenating. The spatial attention is computed as:

$$F' = f^{3 \times 3}([F \otimes F_{sm}; F]), \quad (2)$$

where \otimes denotes element-wise multiplication, and $f^{3 \times 3}$ represents a convolution operation with the filter size of 3×3 . Following the CBAM [35], the channel attention is utilized to focus on “what” is meaningful given an input image by exploiting the inter-channel relationship of the feature. Global pooling is first used to aggregate spatial information of the feature map F' . Then, the fully connected layer is used to connect different channels, as each channel of a feature map is considered as a feature detector [44]. In short, a 1D channel attention map $M_c \in \mathbb{R}^{C \times 1 \times 1}$ can be obtained by feeding the feature map F' into the *GlobalPool-Fc-Relu-Fc-Sigmoid* layers. The final refined output from SAM can be computed as: $F'' = M_c \otimes F'$.

In practice, the predicted skeleton map F_{sm} is downsampled to obtain multi-scale maps (*i.e.*, 1/4, 1/8, 1/16), that are transferred to the regular stream (the thick yellow arrow in Fig. 4 (a)). And then, the extracted feature map (*e.g.*, $C1$) and the corresponding scale skeleton map are used as the input of the Skeleton Attention Module. Note that the proposed Skeleton Attention Module is shared for the high-level and the low-level feature maps (*i.e.*, $C1, C2, C3$).

Skeleton Attention Map and Loss. Given an input sample $(x_i, y_i) \in \{(x_1, y_1), (x_2, y_2), \dots, (x_n, y_n)\}$, where x_i and y_i denote the i -th image and its labels. We use x_i^k to denote the k -th pixel of the i -th training image, with $y_i^k = 0$ for the background and $y_i^k = 1$ for the text pixel. To learn stronger representation of text skeleton, we define the text skeleton ground-truth as a soft label. For the k -th pixel in the text region of i -th image, we first calculate the shortest distance d_i^k between the k -th pixel to its nearest background pixel, and then the value p_i^k is defined as the soft skeleton label of

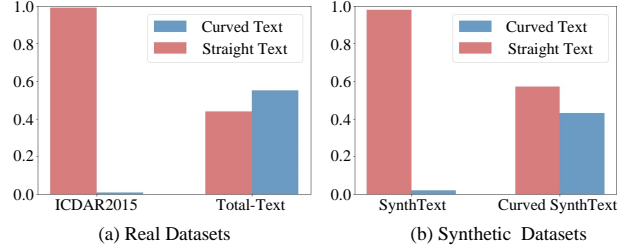


Figure 5: The shape distribution difference between synthetic data and real data causes serious domain gap.

k -th pixel by normalizing d_i^k to $[0, 1]$:

$$p_i^k = \frac{d_i^k}{d_i^*}, \quad (3)$$

where d_i^* is the maximum value of $\{d_i^k\}$ in the i -th image.

Intuitively, the pixels close to the skeleton of the text instance should have a greater value than the boundary pixels (see text skeleton label in Fig. 4 (a)). Since the soft label is a decimal representing the degree of distance, it is incompatible with the commonly binary cross-entropy loss. Besides, the L1 and L2 losses are not sensitive to the distance distribution among $[0, 1]$ [24]. Therefore, to handle the soft label, we modify the cross-entropy loss into a “soft” form. For a pixel x_i^k , p_i^k denotes the value of the k -th pixel in the ground truth skeleton map. \mathcal{F} indicates neural networks. The soft cross-entropy loss for text skeleton loss in Fig. 4 (a) is defined as follows:

$$\mathcal{L}_{ske} = - \sum_k \log(1 - |p_i^k - \mathcal{F}(x_i^k)|), \quad (4)$$

The whole loss function \mathcal{L} for SASN can be expressed as a weighted sum of the loss for the regular stream \mathcal{L}_{ce} (*i.e.*, the commonly binary cross-entropy loss) and the loss for the skeleton stream \mathcal{L}_{ske} :

$$\mathcal{L} = \mathcal{L}_{ce} + \lambda \mathcal{L}_{ske}, \quad (5)$$

where λ is set to 2, which balances the importance between \mathcal{L}_{ske} and \mathcal{L}_{ce} .

3.4. Domain Gap for Synthetic Datasets

Existing real-world text datasets can be divided two types: straight (*e.g.*, ICDAR2015 [11]) and curved (*e.g.*, Total-Text [3]), depending on the shape of the text instance. However, curved synthetic text data are scarce. SynthText [8], as the most widely used synthetic dataset, does not contain curved text, which leads to a considerable domain gap between synthetic data and real data (*e.g.*, Total-Text) in curved text distribution (0.2% *v.s.* 58%), as shown in Fig. 5. Therefore, we also adopt Curved SynthText [18]

Method	Synthetic Data	Evaluation on Total-Text/%		
		P	R	F
BL	SynthText	77.2	73.0	75.0
BL+SA(C1)	SynthText	80.3	73.6	76.8(+1.8)
BL+SA(C1&C2)	SynthText	80.1	74.1	77.1(+2.1)
BL+SA(C1&C2&C3)	SynthText	80.4	74.0	77.1(+2.1)
BL	*SynthText	80.5	73.2	76.7
BL+SA(C1)	*SynthText	81.4	75.5	78.4(+1.7)
BL+SA(C1&C2)	*SynthText	81.0	76.1	78.4(+1.7)
BL+SA(C1&C2&C3)	*SynthText	81.7	75.6	78.5(+1.8)

Table 1: **Multi-Scale features with Skeleton Attention.** ‘SA’, ‘BL’, ‘P’, ‘R’, ‘F’ and ‘*’ refer to ‘Skeleton Attention’, ‘Baseline’, ‘Precision’, ‘Recall’, ‘F-score’ and ‘Curved SynthText [18]’. PSENet [33] is adopted as the detector. The gaps of at least (+1.7%) improvement compared to the baseline are shown in green.

to align the data distribution with curved dataset. In this work, we use SynthText [8] to train SASN for the straight text line and use Curved SynthText [18] to match the curved text line.

4. Experiments

4.1. Datasets and Experimental Settings

Pure Synthetic Datasets. *SynthText* [8] consist of 800k synthetic images generated by adding variants of multi-oriented text with random fonts, size, and color. *Curved SynthText*¹ [18] generates 80m curved texts with character level annotation by revising the text rendering module of the SynthText engine.

Real Datasets. *ICDAR2015* [11] includes 1,000 training and 500 testing images with quadrilateral annotation. *Total-Text*[3] is an English curved text dataset that contains 1,555 images, including 3 different text orientations: horizontal, multioriented, and curved. *MSRA-TD500* [41] consists of 500 training and 200 testing images for detecting multi-lingual long texts of arbitrary orientation. *ICDAR2017-MLT* [22] consists of 18,000 images with texts in 9 languages for multi-lingual text detection. *SCUT-CW1500* [43] is a challenging dataset for curved text detection, which consists of 1,000 training images and 500 test images, and text instances are largely in English and Chinese. *ICDAR2019-ArT* [4] is a large-scale arbitrary-shaped text detection benchmark, and its text regions are labeled by adaptive number of vertices. It consists of 5,603 training images and 4,563 test images. *ICDAR2019-LSVT* [27] includes 450,000 images with text that are freely captured in the streets, e.g., store fronts and landmarks. 50,000 of them are fully annotated and are split into 30,000 images for the training set and 20,000 images for the testing set.

Implementation Details. All of the experiments use

¹<https://github.com/PkuDavidGuan/CurvedSynthText>

Method	Evaluation on Total-Text/%		
	Precision	Recall	F-score
BL	80.5	73.2	76.7
BL+SA(Cha)	79.8	74.0	76.8(+0.1)
BL+SA(Cha&Spa)	80.3	74.6	77.4(+0.7)
BL+SA(Cha&Spa&Skeleton Map)	81.7	75.6	78.5(+1.8)

Table 2: **Combining methods of Skeleton Attention.** ‘SA’, ‘BL’, ‘Cha’ and ‘Spa’ refer to ‘Skeleton Attention’, ‘Baseline’, ‘Channel’ and ‘Spatial’. PSENet [33] is adopted as the detector. In green are the gaps of up to (+1.8%) improvement than baseline.

the same strategy: (1) Training SASN with Curved SynthText based on character annotation, and generating the pixel-level pseudo label on real data based on upright bounding box annotation. (2) Training the detectors (*i.e.*, EAST, PSENet, DB) with the pseudo label. It is worth mentioning that the SASN only needs to train once on Curved SynthText, and we use the same weight to generate pseudo labels on all real benchmarks. Additionally, for all datasets, the threshold for the pseudo-labels generation was the traditional value (*i.e.*, 0.5). The stochastic gradient descent(SGD) optimizer is adopted with a momentum of 0.9 and a weight decay of 0.0005. The batch size is set to 8 per GPU. The learning rate is initialized to 0.02 and decayed with the power of 0.9 for 16 epochs. During training and inference, the crop images are resized to a resolution of 128×128. PSENet [33], EAST [46] and DB [16] are adopted as the base detectors because of their popularity. In the PSENet, EAST and DB experiments, all settings follow the original reports.

4.2. Ablation Study

Here, we conduct two groups of ablation experiments to analyze PF. The ablation study for synthetic data is in supplementary materials

Multi-Scale features with Skeleton Attention. Tab. 1 gives the ablation study about applying the Skeleton Attention on different scale features. Because SA can be applied at different levels for the regular stream, we vary the number of fusion levels from *C1* to *C3* to evaluate the relationship. The method that fuses SA with all level features shows the most significant improvement from 76.7% to 78.5%. Regardless of the used synthetic data and experimental setting, Skeleton Attention can obtain up to 2% improvement compares to the baseline without the attention.

Combining methods of Skeleton Attention. Tab. 2 shows the impact of three submodules: channel attention, spatial attention, and skeleton attention. It is clear that the improvement due to channel attention is limited (*i.e.*, +0.1%), but its spatial attention counterpart contributes to better gain (*i.e.*, +0.7%), the main reason for this may be that spatial information is more important than semantic in-

Method	Annotation	Pre	ICDAR2015/%			MSRA-TD500/%			ICDAR2017-MLT/%			Total-Text/%		
			P	R	F	P	R	F	P	R	F	P	R	F
<i>Strong Supervision</i>														
CTPN[29]	GT	-	74.2	51.6	60.9	-	-	-	-	-	-	-	-	-
SegLink[26]	GT	✓	73.1	76.8	75.0	86.0	70.0	77.0	-	-	-	30.3	23.8	26.7
EAST[46]	GT	-	80.5	72.8	76.4	81.7	61.6	70.2	-	-	-	-	-	-
PixelLink[6]	GT	-	82.9	81.7	82.3	83.0	73.2	77.8	-	-	-	-	-	-
TextSnake[19]	GT	✓	84.9	80.4	82.6	83.2	73.9	78.3	-	-	-	82.7	74.5	78.4
PSENet[33]	GT	-	81.5	79.7	80.6	-	-	-	73.7	68.2	70.8	81.8	75.1	78.3
PSENet[33]	GT	✓	86.9	84.5	85.7	-	-	-	-	-	-	84.0	78.0	80.9
EAST [†]	GT	-	76.9	77.1	77.0	71.8	69.1	70.4	68.1	63.2	65.6	-	-	-
EAST [†]	GT	✓	82.0	82.4	82.2	77.9	76.5	77.2	70.3	62.8	66.4	-	-	-
PSENet [†]	GT	-	81.6	79.5	80.5	80.6	77.7	79.1	73.1	67.3	70.1	80.4	76.5	78.4
PSENet [†]	GT	✓	86.4	84.0	85.2	84.1	85.0	84.5	72.5	69.1	70.8	83.4	78.1	80.7
<i>Weakly Supervision</i>														
EAST	b-GT	-	65.8	63.8	64.8	40.5	31.1	35.2	66.3	59.6	62.8	-	-	-
EAST+PF	PL	-	77.8	78.2	78.0	71.3	70.2	70.7	67.3	64.1	65.7	-	-	-
EAST	b-GT	✓	70.8	72.0	71.4	48.3	42.4	45.2	67.2	60.1	63.5	-	-	-
EAST+PF	PL	✓	81.3	82.2	81.8	77.4	75.5	76.4	67.6	64.9	66.3	-	-	-
PSENet	b-GT	-	70.2	69.1	69.6	47.2	36.9	41.4	67.2	61.4	64.2	46.5	43.6	45.0
PSENet+PF	PL	-	82.9	77.6	80.2	80.3	77.5	78.9	72.4	69.3	70.8	81.7	75.6	78.5
PSENet	b-GT	✓	72.7	74.3	73.5	47.5	39.5	43.1	66.4	63.1	64.7	51.9	47.5	49.6
PSENet+PF	PL	✓	86.8	84.2	85.5	84.4	84.7	84.5	73.8	67.7	70.6	82.6	78.4	80.5

Table 3: **The results of Polygon-free on ICDAR2015, MSRA-TD500, ICDAR2017-MLT, Total-Text.** † refers to our testing performance. The ‘GT’, ‘b-GT’ and ‘PL’ refer to the ‘Ground Truth’, ‘Upright Bounding Box Annotation of Ground Truth’ and ‘Pseudo Label from SASN’, respectively. ‘P’, ‘R’, ‘F’ and “Pre” refer to ‘Precision’, ‘Recall’, ‘F-score’ and ‘pre-training on SynthText’, respectively. In green (strong supervision) and in bold (Polygon-free) are highlighted for comparison.

formation for text segmentation task. Another important contribution is the soft attention weight map (*i.e.*, Skeleton Map), the performance achieves further improvement (*i.e.*, +1.8%) after using the Skeleton Map. This is in line with our expectations, and we argue that the text skeleton is vital because of its high representation power.

Method	Annotation	ICDAR2019-LSVT/%		
		P	R	F
<i>Strong Supervision</i>				
EAST*	GT	71.7	77.6	74.5
PSENet [†]	GT	80.9	74.2	77.4
<i>Weakly Supervision</i>				
EAST	b-GT	60.3	52.2	56.0
EAST+PF	PL	73.0	76.1	74.5(+18.5)
PSENet	b-GT	62.1	53.2	57.3
PSENet+PF	PL	80.1	75.3	77.6(+20.3)

Table 4: **The results on ICDAR2019-LSVT.** * are collected from [27]. ‘GT’, ‘b-GT’ and ‘PL’ refer to ‘Ground Truth’, ‘Upright Bounding Box Annotation’ and ‘Pseudo Label from SASN’, respectively. ‘P’, ‘R’ and ‘F’ refer to ‘Precision’, ‘Recall’ and ‘F-score’. The gaps of at least (+18.5%) improvement after using BF are shown in green.

4.3. Experiments on Scene Text Detection

In this section, we present the experiments for Polygon-free on seven datasets, and ICDAR2019-Art and CTW1500 are given in the supplementary material.

4.3.1 Quadrilateral-type datasets

Tab. 3 lists the experimental results for various methods on the ICDAR2015, ICDAR2017 and MSRA-TD500 datasets, and the ICDAR2019-LSVT is shown in Tab. 4.

For *ICDAR2015* [11], PSENet [33] using pseudo label achieves **almost the same performance** (85.5% v.s. 85.2%) with that using ground truth, proving the high quality of the pseudo label generated by PF. By contrast, direct training the detector with upright bounding box annotation obtains an unsatisfactory F-score (73.5%), with a performance gap of more than 10%. EAST [46] shows similar performance (81.8% vs. 82.2%) to that of PSENet. Moreover, without pretraining on SynthText, the F-score (78.0%) obtained using the pseudo label shows a 1.0% improvement over that (77.0%) of using ground truth.

For *MSRA-TD500* [41], annotations are provided at the line level, including the spaces between the words in the box. Therefore, bounding box annotation on MSRA-TD500 usually contains a large background, causing poor performance (35.2% for EAST and 41.4% for PSENet). In this case, the pseudo label from SASN still obtains almost the same performance (70.7% for EAST and 78.9% for PSENet without pre-trained model) as that (70.4% for EAST and 79.1% for PSENet) of polygon annotation. With the pre-trained model, a similar result is obtained, and PSENet with pseudo label (84.5%) achieves a huge improvement (+41.4%) compared to training directly with up-



Figure 6: **Comparison of pseudo label and manual label on Total-Text [3].** Pseudo label is more smooth than the manual label.

right bounding box (43.1%).

For *ICDAR2017-MLT* [22], the performance is similar to ICDAR15, and pseudo label shows strongly improved performance compared to that using ground truth. The difference is that the upright bounding box also leads to relatively good performance (62.8% for EAST and 64.2% for PSENet). The main reason for this is that the texts in ICDAR2017-MLT have a small tilting angle and size.

Tab. 4 gives the results for *ICDAR2019-LSVT* [27]. With pseudo label from SASN, PSENet achieves 77.6% F-score, **20.3%** better than training directly with upright bounding box annotation, and almost the same as that obtained using original polygon annotation (77.4%). A similar case with **18.5%** performance improvements for EAST. For large-scale ICDAR2019-LSVT with **50k** images, the excellent performance has great significance for reducing the annotation cost, and for the first time, the great potential of box-supervised text detection is revealed.

4.3.2 Curved-type dataset

For *Total-Text* [3], Tab. 3 lists the experimental results. The annotation on Total-Text is complex and polygonal in shape. The **great performance** (80.5%) of Polygon-free further demonstrates the significance of our work, and Fig. 7 provides some visualization of ground truth and pseudo label. Similar to MSRA-TD500, the upright bounding box annotation on Total-Text also contains plenty of backgrounds, causing poor performance (45.0% and 49.6%). The use of the pseudo label generated by SASN can still achieve excellent performance (78.5% and 80.5%) with improvements of **33.5%** and **30.9%**.

4.4. Discussion

Weakly supervision v.s. Strong supervision. To further present the effectiveness of the Polygon-free, we summarized the results concerning three detectors (*i.e.*, PSENet [33], EAST [46] and DB [16]) and seven datasets (*i.e.*, ICDARs, Total-Text, CTW1500 and MSRA-TD500) to Table 5. As a **plug-and-play** weakly-supervised approach, the F1 of PF can achieve 6.6% ~ 35.5% improvements than directly training with upright bounding box (two points), almost equal to strong-supervised methods on all

Datasets	Cited	Methods	F1 [▲] /%	F1 [★] /%	F1 [†] /%
ICDAR2015	624	EAST	64.8	78.0 (+13.2)	76.4
		PSENet	73.5	85.5 (+12.0)	85.7
MSRA-TD500	630	EAST	35.2	70.7 (+35.5)	70.2
ICDAR2017MLT	128	PSENet	64.2	70.8 (+6.6)	70.8
		PSENet	49.6	80.5 (+30.9)	80.9
Total-Text	142	DB	49.1	84.5(+35.4)	84.7
		PSENet	47.6	81.5(+33.9)	82.2
CTW1500	105	PSENet	47.6	81.5(+33.9)	82.2
ICDAR2019LSVT	6	PSENet	57.3	77.6(+20.3)	77.4
ICDAR2019ArT	13	PSENet	46.6	69.2(+22.6)	69.5

Table 5: **Weakly supervision v.s. Strong supervision.**

▲, ★ and † refer to ‘Upright Bounding Box Annotation’, ‘Polygon-free(ours)’ and ‘Original Paper Report or our testing result (strong supervision)’. In blue are the gaps of at least (+6.6%) improvement after using PF.



Figure 7: **Visualization for the pseudo labels from Polygon-free.** The images are from Total-Text [3].

datasets. This means that the proposed method can be directly applied for industry application with a little loss (*i.e.*, < 0.5%) of performance. The competitive performance of PF proves the practicability efficiency of the pseudo label. Fig. 7 gives some visualization of the pseudo label.

Pseudo Label v.s. Manual Label. With the ideal condition, compared with the pseudo label, the manual label is more accurate. However, since many factors such as disagreement from multiple annotators, there are many label errors or low-quality manual labels. As shown in Fig. 6 (the first row), manual labels even can not contain the whole text region, which will cause serious inference for the following recognition task. As the number of data increases, it is more difficult to assure data quality, and even high-quality datasets are likely to contain incorrect labels. By contrast, in these cases, the pseudo label is more **smooth** for suiting each character, which can obtain a better performance via supervising the network. Besides, we argue that Polygon-free can be used in other tasks to boost their efficiency. For example, designing an automatic annotation tool with PF, more smooth and high-quality annotation can be obtained by handling some bad cases at a low cost.

5. Conclusion

In this paper, we present a simple but surprisingly effective and practical system termed Polygon-free, in which most existing polygon-based text detectors are trained with only upright bounding box annotations. The core contribution is to transfer knowledge from synthetic data to real data to enhance the supervision information via a skeleton attention segmentation network. The experiments showed that our method achieves almost the same performance as that of strong supervision while saving huge annotation cost (e.g., 80% + data cost on Total-Text), which can provide a new perspective for weakly supervised text detection and save much money for for real-world application.

References

- [1] Youngmin Baek, Bado Lee, Dongyoon Han, Sangdoon Yun, and Hwalsuk Lee. Character region awareness for text detection. In *Proceedings of the IEEE Conference on Computer Vision and Pattern Recognition*, pages 9365–9374, 2019. 2
- [2] Long Chen, Hanwang Zhang, Jun Xiao, Liqiang Nie, Jian Shao, Wei Liu, and Tat-Seng Chua. Sca-cnn: Spatial and channel-wise attention in convolutional networks for image captioning. In *Proceedings of the IEEE conference on computer vision and pattern recognition*, pages 5659–5667, 2017. 2
- [3] Chee Kheng Ch'ng and Chee Seng Chan. Total-text: A comprehensive dataset for scene text detection and recognition. In *Proc. Int. Conf. Document Analysis Recogn.*, pages 935–942, 2017. 1, 2, 5, 6, 8
- [4] Chee Kheng Chng, Yuliang Liu, Yipeng Sun, Chun Chet Ng, Canjie Luo, Zihan Ni, ChuanMing Fang, Shuaitao Zhang, Junyu Han, Errui Ding, et al. Icdar2019 robust reading challenge on arbitrary-shaped text-rrc-art. In *ICDAR2019*, pages 1571–1576. IEEE, 2019. 2, 6
- [5] Jifeng Dai, Kaiming He, and Jian Sun. Boxesup: Exploiting bounding boxes to supervise convolutional networks for semantic segmentation. In *Proceedings of the IEEE international conference on computer vision*, pages 1635–1643, 2015. 2, 3
- [6] Dan Deng, Haifeng Liu, Xuelong Li, and Deng Cai. Pixelink: Detecting scene text via instance segmentation. In *Proc. AAAI Conf. Artificial Intell.*, pages 6773–6780, 2018. 7
- [7] Ankush Gupta, Andrea Vedaldi, and Andrew Zisserman. Synthetic data for text localisation in natural images. In *Proc. IEEE Conf. Comp. Vis. Patt. Recogn.*, pages 2315–2324, 2016. 2, 4
- [8] Ankush Gupta, Andrea Vedaldi, and Andrew Zisserman. Synthetic data for text localisation in natural images. In *Proceedings of the IEEE conference on computer vision and pattern recognition*, pages 2315–2324, 2016. 5, 6
- [9] Kaiming He, Xiangyu Zhang, Shaoqing Ren, and Jian Sun. Deep residual learning for image recognition. In *Proceedings of the IEEE conference on computer vision and pattern recognition*, pages 770–778, 2016. 4
- [10] Han Hu, Chengquan Zhang, Yuxuan Luo, Yuzhuo Wang, Junyu Han, and Errui Ding. Wordsup: Exploiting word annotations for character based text detection. In *Proceedings of the IEEE International Conference on Computer Vision*, pages 4940–4949, 2017. 3
- [11] Dimosthenis Karatzas, Lluís Gomez-Bigorda, Angelos Nicolaou, Suman Ghosh, Andrew Bagdanov, Masakazu Iwamura, Jiri Matas, Lukas Neumann, Vijay Ramaseshan Chandrasekhar, Shijian Lu, et al. Icdar 2015 competition on robust reading. In *Proc. Int. Conf. Document Analysis Recogn.*, pages 1156–1160, 2015. 4, 5, 6, 7
- [12] Anna Khoreva, Rodrigo Benenson, Jan Hosang, Matthias Hein, and Bernt Schiele. Simple does it: Weakly supervised instance and semantic segmentation. In *Proceedings of the IEEE conference on computer vision and pattern recognition*, pages 876–885, 2017. 3
- [13] Viveka Kulharia, Siddhartha Chandra, Amit Agrawal, Philip Torr, and Amrith Tyagi. Box2seg: Attention weighted loss and discriminative feature learning for weakly supervised segmentation. In *European Conference on Computer Vision*, pages 290–308. Springer, 2020. 2, 3
- [14] Zhuang Li, Weijia Wu, Mike Zheng Shou, Jiahong Li, Size Li, Zhongyuan Wang, and Hong Zhou. Contrastive learning of semantic and visual representations for text tracking. *arXiv preprint arXiv:2112.14976*, 2021. 1
- [15] Minghui Liao, Baoguang Shi, Xiang Bai, Xinggong Wang, and Wenyu Liu. Textboxes: A fast text detector with a single deep neural network. In *Proc. AAAI Conf. Artificial Intell.*, pages 4161–4167, 2017. 1, 2
- [16] Minghui Liao, Zhaoyi Wan, Cong Yao, Kai Chen, and Xiang Bai. Real-time scene text detection with differentiable binarization. In *AAAI*, pages 11474–11481, 2020. 1, 2, 6, 8
- [17] Jonathan Long, Evan Shelhamer, and Trevor Darrell. Fully convolutional networks for semantic segmentation. In *Proc. IEEE Conf. Comp. Vis. Patt. Recogn.*, pages 3431–3440, 2015. 2
- [18] Shangbang Long, Yushuo Guan, Bingxuan Wang, Kaigui Bian, and Cong Yao. Rethinking irregular scene text recognition. *arXiv*, pages arXiv–1908, 2019. 5, 6
- [19] Shangbang Long, Jiaqiang Ruan, Wenjie Zhang, Xin He, Wenhao Wu, and Cong Yao. Textsnake: A flexible representation for detecting text of arbitrary shapes. *Proc. Eur. Conf. Comp. Vis.*, pages 20–36, 2018. 1, 2, 7
- [20] Shangbang Long and Cong Yao. Unrealtext: Synthesizing realistic scene text images from the unreal world. *arXiv preprint arXiv:2003.10608*, 2020. 2
- [21] Pengyuan Lyu, Minghui Liao, Cong Yao, Wenhao Wu, and Xiang Bai. Mask textspotter: An end-to-end trainable neural network for spotting text with arbitrary shapes. In *Proc. Eur. Conf. Comp. Vis.*, pages 67–83, 2018. 1, 2
- [22] Nibal Nayef, Fei Yin, Imen Bizid, Hyunsoo Choi, Yuan Feng, Dimosthenis Karatzas, Zhenbo Luo, Umapada Pal, Christophe Rigaud, Joseph Chazalon, et al. Icdar2017 robust reading challenge on multi-lingual scene text detection and script identification-rrc-mlt. In *ICDAR2017*. IEEE, 2017. 6, 8
- [23] Jordi Pont-Tuset, Pablo Arbelaez, Jonathan T Barron, Ferran Marques, and Jitendra Malik. Multiscale combinatorial

- grouping for image segmentation and object proposal generation. *IEEE transactions on pattern analysis and machine intelligence*, 39(1):128–140, 2016. [2](#), [3](#)
- [24] Shaoqing Ren, Kaiming He, Ross Girshick, and Jian Sun. Faster r-cnn: Towards real-time object detection with region proposal networks. In *Proc. Advances in Neural Inf. Process. Syst.*, pages 91–99, 2015. [2](#), [5](#)
- [25] Carsten Rother, Vladimir Kolmogorov, and Andrew Blake. ” grabcut” interactive foreground extraction using iterated graph cuts. *ACM transactions on graphics (TOG)*, 23(3):309–314, 2004. [2](#), [3](#)
- [26] Baoguang Shi, Xiang Bai, and Serge Belongie. Detecting oriented text in natural images by linking segments. In *Proc. IEEE Conf. Comp. Vis. Patt. Recogn.*, pages 2550–2558, 2017. [7](#)
- [27] Yipeng Sun, Jiaming Liu, Wei Liu, Junyu Han, Errui Ding, and Jingtuo Liu. Chinese street view text: Large-scale chinese text reading with partially supervised learning. In *ICCV*, pages 9086–9095, 2019. [1](#), [2](#), [6](#), [7](#), [8](#)
- [28] Shangxuan Tian, Shijian Lu, and Chongshou Li. Wetext: Scene text detection under weak supervision. In *Proceedings of the IEEE International Conference on Computer Vision*, pages 1492–1500, 2017. [3](#)
- [29] Zhi Tian, Weilin Huang, Tong He, Pan He, and Yu Qiao. Detecting text in natural image with connectionist text proposal network. In *Proc. Eur. Conf. Comp. Vis.*, pages 56–72, 2016. [1](#), [2](#), [7](#)
- [30] Zhi Tian, Chunhua Shen, and Hao Chen. Conditional convolutions for instance segmentation. *arXiv preprint arXiv:2003.05664*, 2020. [3](#)
- [31] Zhi Tian, Chunhua Shen, Xinlong Wang, and Hao Chen. Boxinst: High-performance instance segmentation with box annotations. *arXiv preprint arXiv:2012.02310*, 2020. [3](#)
- [32] Mei Wang and Weihong Deng. Deep visual domain adaptation: A survey. *Neurocomputing*, 312:135–153, 2018. [4](#)
- [33] Wenhai Wang, Enze Xie, Xiang Li, Wenbo Hou, Tong Lu, Gang Yu, and Shuai Shao. Shape robust text detection with progressive scale expansion network. In *Proc. IEEE Conf. Comp. Vis. Patt. Recogn.*, pages 9336–9345, 2019. [1](#), [2](#), [3](#), [6](#), [7](#), [8](#)
- [34] Wenhai Wang, Enze Xie, Xiaoge Song, Yuhang Zang, Wenjia Wang, Tong Lu, Gang Yu, and Chunhua Shen. Efficient and accurate arbitrary-shaped text detection with pixel aggregation network. In *Proc. IEEE Int. Conf. Comp. Vis.*, pages 8440–8449, 2019. [1](#), [3](#)
- [35] Sanghyun Woo, Jongchan Park, Joon-Young Lee, and In So Kweon. Cbam: Convolutional block attention module. In *Proceedings of the European conference on computer vision (ECCV)*, pages 3–19, 2018. [2](#), [3](#), [4](#), [5](#)
- [36] Weijia Wu, Ning Lu, Enze Xie, Yuxing Wang, Wenwen Yu, Cheng Yang, and Hong Zhou. Synthetic-to-real unsupervised domain adaptation for scene text detection in the wild. In *Proceedings of the Asian Conference on Computer Vision*, 2020. [1](#)
- [37] Weijia Wu, Jici Xing, and Hong Zhou. Textcohesion: Detecting text for arbitrary shapes. *arXiv preprint arXiv:1904.12640*, 2019. [1](#)
- [38] Weijia Wu, Debing Zhang, Yuanqiang Cai, Sibao Wang, Jiahong Li, Zhuang Li, Yejun Tang, and Hong Zhou. A bilingual, openworld video text dataset and end-to-end video text spotter with transformer. In *Thirty-fifth Conference on Neural Information Processing Systems Datasets and Benchmarks Track (Round 2)*, 2021. [1](#)
- [39] Weijia Wu, Debing Zhang, Ying Fu, Chunhua Shen, Hong Zhou, Yuanqiang Cai, and Ping Luo. End-to-end video text spotting with transformer. *arXiv preprint arXiv:2203.10539*, 2022. [1](#)
- [40] Yongchao Xu, Yukang Wang, Wei Zhou, Yongpan Wang, Zhibo Yang, and Xiang Bai. Textfield: Learning a deep direction field for irregular scene text detection. *IEEE Transactions on Image Processing*, 28(11):5566–5579, 2019. [2](#)
- [41] Cong Yao, Xiang Bai, Wenyu Liu, Yi Ma, and Zhuowen Tu. Detecting texts of arbitrary orientations in natural images. In *Proc. IEEE Conf. Comp. Vis. Patt. Recogn.*, pages 1083–1090, 2012. [6](#), [7](#)
- [42] Liu Yuliang, Jin Lianwen, Zhang Shuaitao, and Zhang Sheng. Detecting curve text in the wild: New dataset and new solution. *arXiv preprint arXiv:1712.02170*, 2017. [1](#)
- [43] Liu Yuliang, Jin Lianwen, Zhang Shuaitao, and Zhang Sheng. Detecting curve text in the wild: New dataset and new solution. *arXiv preprint arXiv:1712.02170*, 2017. [6](#)
- [44] Matthew D Zeiler and Rob Fergus. Visualizing and understanding convolutional networks. In *European conference on computer vision*, pages 818–833. Springer, 2014. [5](#)
- [45] Zheng Zhang, Chengquan Zhang, Wei Shen, Cong Yao, Wenyu Liu, and Xiang Bai. Multi-oriented text detection with fully convolutional networks. In *Proc. IEEE Conf. Comp. Vis. Patt. Recogn.*, pages 4159–4167, 2016. [2](#)
- [46] Xinyu Zhou, Cong Yao, He Wen, Yuzhi Wang, Shuchang Zhou, Weiran He, and Jiajun Liang. East: an efficient and accurate scene text detector. In *Proc. IEEE Conf. Comp. Vis. Patt. Recogn.*, pages 5551–5560, 2017. [1](#), [2](#), [4](#), [6](#), [7](#), [8](#)